Effective reduction of magnetisation losses in copper-plated multifilament coated conductors using spiral geometry

OPEN ACCESS
IOP Publishing
Superconductor Science and Technology
Supercond. Sci. Technol. **35** (2022) 025003 (13pp)
https://doi.org/10.1088/1361-6668/ac3f9c

Effective reduction of magnetisation losses in copper-plated multifilament coated conductors using spiral geometry

Naoyuki Amemiya[1,*], Mao Shigemasa[1], Akira Takahashi[1], Ning Wang[1], Yusuke Sogabe[1], Satoshi Yamano[2,3] and Hisaki Sakamoto[2]

[1] Department of Electrical Engineering, Graduate School of Engineering, Kyoto University, Kyoto-Daigaku-Katsura, Nishikyo, Kyoto 615-8510, Japan
[2] Furukawa Electric Co., Ltd., 2-6-4 Otemachi, Chiyoda, Tokyo 100-8322, Japan
[3] SuperPower Inc., 21 Airport Road, Glenville, NY 12302, United States of America

E-mail: amemiya.naoyuki.6a@kyoto-u.ac.jp

Received 4 October 2021, revised 5 November 2021
Accepted for publication 2 December 2021
Published 31 December 2021

Abstract

We wound copper-plated multifilament coated conductors spirally on a round core to decouple filaments electromagnetically under ac transverse magnetic fields and measured their magnetisation losses. Although the coated conductors were plated with copper, which connects all filaments electrically and allows current sharing among them, the spiral geometry decoupled filaments similar to the twist geometry, and the magnetisation loss was reduced effectively by the multifilament structure. The measured magnetisation loss of a 4 mm wide, 10-filament coated conductor with a 20 μm thick copper wound spirally on a 3 mm core was only 7% of that of the same 10-filament coated conductor with a straight shape under an ac transverse magnetic field with an amplitude and frequency of 100 mT and 65.44 Hz, respectively. We separated the measured magnetisation losses into hysteresis and coupling losses and discussed the influence of filament width, copper thickness, and core diameter on both losses. We compared the hysteresis losses with the analytical values given by Brandt and Indenbom and compared the coupling losses with the values calculated using a general expression of coupling loss with the coupling time constants and geometry factors.

Keywords: ac loss, CORC®, magnetisation loss, multifilament, SCSC cable, spiral, striation

(Some figures may appear in colour only in the online journal)

* Author to whom any correspondence should be addressed.

1. Introduction

Small magnetisation losses under ac transverse magnetic fields and protection as well as stability against normal transition are keys to the various power applications of coils wound with coated conductors. In principle, by striating the wide superconductor layer of a coated conductor to form narrower filaments, magnetisation loss can be reduced [1–17], and insulating the filaments electrically from one another might be ideal for this purpose.

However, note that filaments must be electrically connected to one another at both terminals of a conductor in a real coil in order to feed a current. In such a case, we must transpose filaments to decouple against an ac transverse magnetic field and, then, to reduce the magnetisation loss. Šouc *et al* wound multifilament coated conductors spirally on a round core to transpose filaments and demonstrated significant reduction in magnetisation loss [18]. However, the lack of a stabilisation layer, such as copper, is a concern in similar multifilament coated conductors to the ones shown in figure 1(a). Copper plating is a popular approach to improve the stability of coated conductors and to help their protection. Several groups have applied this approach to multifilament coated conductors [13–15]. Most of them did not connect filaments electrically using copper, as shown in figure 1(b), to avoid electromagnetic coupling among filaments, which affects magnetisation loss reduction by the multifilament structure. Vojenčiak *et al* striated the superconductor layers of coated conductors through their copper layers using a laser to form filaments, fabricated conductor on round core (CORC®) cables using such coated conductors, and demonstrated magnetisation loss reduction compared to reference cables fabricated using monofilament coated conductors [14]. Similar experiments were reported by Li *et al* [19] and Goo *et al* [20]. All of these previous studies used multifilament coated conductors with a copper stabilising layer that does not electrically connect filaments, as shown in figure 1(b).

Meanwhile, electrical connection among filaments through copper is preferable for stability and protection, because it enables the detour of current to avoid the local normal section (an intrinsic defect or a normal-transiting part) of a filament. Such a current detour is known as current sharing. Note that a local defect in a filament can block the current in the filament, which is insulated from the others. If there is one local defect in each narrow insulated filament in a long multifilament coated conductor, the conductor cannot carry any current. If we plate the entire group of filaments with copper, as shown in figure 1(c), the copper connects all filaments electrically and allows current sharing [15–17]. In this paper, we call this type of conductor a *copper-plated multifilament (or striated) coated conductor*. The drawback of this type of conductor is the electromagnetic coupling of filaments under ac transverse magnetic fields by the coupling current flowing through the copper, which could increase the magnetisation loss [15]. To reduce the magnetisation loss effectively, the coupling time constant, which is the decay time constant of the coupling current, must be much shorter than the characteristic time of the magnetic field change. The coupling time constants are quite large even in low-T_c superconductor (LTS)

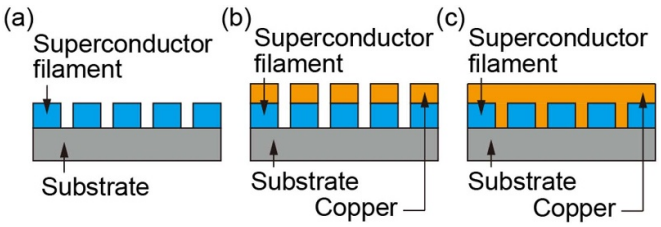

Figure 1. Multifilament coated conductors with and without a copper stabilising layer: (a) without copper stabilising layer, (b) with copper stabilising layer on each filament, which does not connect filaments electrically, and (c) copper stabilising layer covers entire group of filaments, which connects all filaments electrically.

wires unless they are not twisted, but we can twist round metallic LTS wires to reduce their coupling time constants. We previously conducted proof-of-concept experiments on the reduction of coupling time constants of copper-plated multifilament coated conductors using spiral geometry, that is, CORC-like geometry. In the experiments, we wound coated conductors with a 100 μm thick substrate loosely on round cores with relatively large diameters (10–20 mm) [21]. The spiral geometry successfully played a role equivalent to that of the twist geometry in reducing the coupling time constants.

Up-to-date CORC® wires are wound on cores with a diameter of 2.5 mm [22, 23], and the symmetric tape round (STAR) wires are wound on even smaller cores [24, 25]. If we wind a copper-plated multifilament coated conductor spirally on a core with such a small diameter with a sufficiently short pitch, we can reduce its coupling time constant significantly, as explained in section 2 [26–28]. Based on this consideration, we have proposed the concept of a *spiral copper-plated striated coated-conductor cable* (*SCSC cable*) (also called as *'double SC' cable*), as shown in figure 2, in which we wind copper-plated striated (multifilament) coated conductors spirally on a round core [26, 27][4]. The copper improves the stability and helps the protection whereas the spiral geometry decouples filaments against ac transverse magnetic fields, thus effectively reducing magnetisation losses. The configuration of the superconducting elements (thin strips twisted around a core) in the SCSC cable is almost identical to the filament configuration in classical LTS wires. Consideration on ac losses and reduction strategies (finer filaments, shorter twist pitches, and higher transverse resistivity) are therefore similar.

A drawback of the SCSC cables is the reduction in engineering and winding pack current density. However, it should be noted that reasonably high engineering current densities were reported for the CORC® wires [22, 23] and the STAR wires [24, 25] whose spiral structures are same as those of the SCSC cables.

The objective of this study is to demonstrate the magnetisation-loss reduction of *copper-plated multifilament*

[4] Some authors called such cables CORC cables consisting of multifilament coated conductors. We avoid calling our cable CORC cable, because CORC® is a trademark. In this paper, we use *spiral multifilament coated conductor* as a common terminology, whereas we call our cable consisting of *copper-plated* multifilament coated conductor SCSC cable.

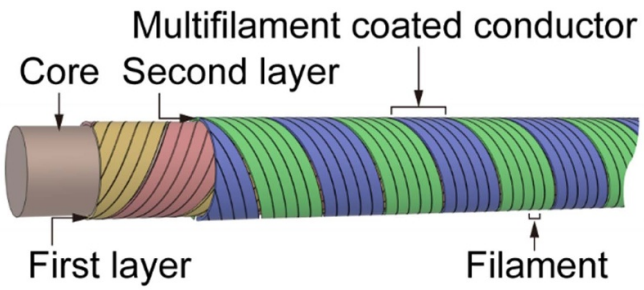

Figure 2. Schematic view of the SCSC cable.

coated conductors subjected to ac transverse magnetic fields using the spiral geometry. Note that we reduced the core diameter to 3 mm to decrease the coupling time constant. We also aim to clarify the details of the coupling and hysteretic loss characteristics of copper-plated multifilament coated conductors wound spirally on round cores (hereafter, *spiral copper-plated multifilament coated conductors*), such as the influence of their filament width, copper thickness, and core diameter. To achieve these objectives, we prepared copper-plated multifilament coated conductors with a 30 μm thick substrate, wound them spirally on round cores with diameters of 3 and 5 mm, and measured their magnetisation losses.

The remainder of this paper is organised as follows. First, we explain the effect of spiral geometry on decoupling filaments in a copper-plated multifilament coated conductor in section 2. Section 3 describes the specifications of the coated conductors and their spiral geometries, and section 4 describes the experimental method. Section 5 presents and discusses the results. We compare the magnetisation losses of straight and spiral samples made with copper-plated multifilament and monofilament coated conductors. Then, we separate the measured magnetisation loss into frequency-independent and frequency-dependent components and examine their detailed characteristics. The former component primarily corresponds to hysteresis loss, whereas the latter component includes coupling and eddy current losses. Finally, section 6 presents our conclusions.

2. Spiral geometry of copper-plated multifilament coated conductor to decouple filaments

A method that is equivalent to twisting in LTS wires to reduce coupling time constants [29, 30] is required to reduce magnetisation losses effectively in practical long copper-plated multifilament coated conductors.

Figure 3(a) shows a schematic side view of the coupling currents in a spiral copper-plated multifilament coated conductor. D and L_p denote the diameter and pitch of the spiral coated conductor, respectively:

$$L_\mathrm{p} = \frac{\pi D}{\tan\alpha} \tag{1}$$

where α is the angle between the coated conductor and the core axis. As shown in this figure, when the spiral copper-plated multifilament coated conductor is subjected to an ac transverse magnetic field, the coupling current is confined to every half spiral pitch, because the orientation of the tape (coated conductor) faces against the magnetic field is inverted every half spiral pitch. In figure 3(b), we unwind the spiral copper-plated multifilament coated conductor and put it on a flat plane. In terms of coupling currents, figure 3(b) is equivalent to figure 3(a), where L_p1 denotes the length of the section of the coated conductor corresponding to a single spiral pitch L_p:

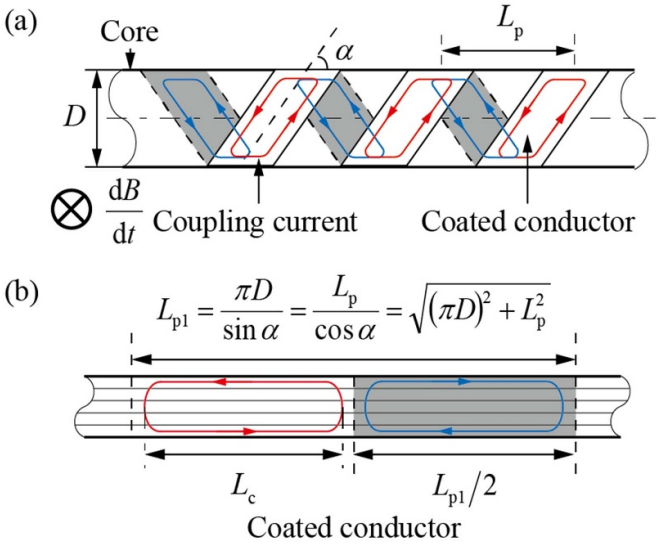

Figure 3. Schematic view of coupling currents in a spiral copper-plated multifilament coated conductor: (a) side view and (b) the coated conductor unwound and put on a flat plane.

$$L_\mathrm{p1} = \sqrt{(\pi D)^2 + L_\mathrm{p}^2} = \frac{L_\mathrm{p}}{\cos\alpha} = \frac{\pi D}{\sin\alpha}. \tag{2}$$

Because the length of the coupling current L_c is restricted to $L_\mathrm{p1}/2$ as shown in figure 3(b), the coupling time constant, which is proportional to the square of its length in principle, is proportional to the square of $L_\mathrm{p1}/2$. Whereas the coupling current expands to the entire length L_t in a straight copper-plated multifilament coated conductor, as shown in figure 4(a), it is confined to each half pitch $L_\mathrm{p1}/2$ and is independent of L_t in a spiral copper-plated multifilament coated conductor, as shown in figure 4(b). This is the principle by which the spiral geometry reduces the coupling time constant and decouples filaments [21].

3. Coated conductors used in experiments and spiral geometries

Furukawa Electric Co., Ltd. and SuperPower Inc. fabricated the coated conductors used in the experiments. A schematic cross section is shown in figure 5. Their 30 μm thick HASTELLOY® substrate allows us to wind them on core with small diameters. The superconductor layer with a silver protective layer was striated by a laser to form filaments, covered with an additional silver layer, and subsequently plated with copper. The striations between the superconductor filaments were filled with copper. The superconductor filaments were connected electrically by the copper filled in the striations

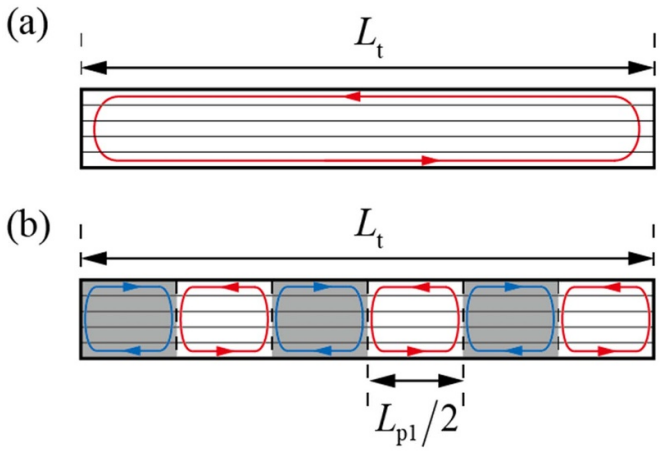

Figure 4. Coupling currents in copper-plated multifilament coated conductors: (a) straight coated conductor, in which coupling current expands to its entire length L_t and (b) spiral coated conductor, in which coupling current is confined to each half pitch $L_{p1}/2$ and is independent of L_t.

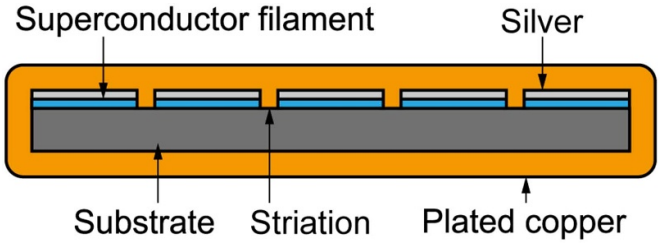

Figure 5. Schematic cross section of copper-plated multifilament coated conductor.

between them and by the copper covering them. We prepared variations of multifilament coated conductors and reference monofilament coated conductors, whose detailed specifications are listed in table 1. Comparing the critical currents of the monofilament coated conductors (B2-a2, B3-a1, and B3-a2) with multifilament coated conductors (the others), we find that the losses of critical currents by striation are at an acceptable level.

We wound each coated conductor listed in table 1 spirally on a round glass fibre-reinforced plastic core with a diameter D_c of 3 or 5 mm, so that the superconductor layer and the substrate of the coated conductor face inside and outside, respectively. This orientation is favourable for preventing critical current degradation, as reported for CORC wires [23], which use coated conductors with the same substrate thickness (30 μm) and a core diameter of 2.5 mm. We measured the critical current of a monofilament coated conductor wound spirally on 3 mm core with α of 55° and confirmed that the critical current was not degraded by the winding. Because the number of layers is one, we assume that D in equations (1) and (2) is equal to D_c. The specifications of the spiral copper-plated coated conductors for magnetisation loss measurements are listed in table 2 together with those of the reference straight copper-plated coated conductors. The pictures of spiral copper-plated multifilament coated conductors are shown in figure 6.

4. Experimental method

We measured the magnetisation losses Q_m of the samples cooled in liquid nitrogen (77 K) using our ac loss measurement systems, the schematic of which is shown in figure 7 [16, 31, 32]. Note that we describe magnetisation loss using the energy dissipated in the unit length of a coated conductor per cycle of magnetic field change, whose unit is J m^{-1}. AC transverse magnetic fields with sinusoidal waveforms were applied to a sample using a copper magnet, and the magnetisation losses were measured using a pickup coil [31]. The empty compensation coil, whose geometry is identical to that of the pickup coil, was connected in series to the pickup coil to suppress the inductive voltage component. We conducted two types of experiments using two ac loss measurement systems with different operational conditions.

In most of the experiments reported in this paper, the amplitude of the applied magnetic field $\mu_0 H_m$ was varied from 1 to 100 mT, but its frequency f was discrete (13.38, 26.62, 65.44, and 112.5 Hz), because capacitors were used to compensate for the large inductive voltage of the magnet.

In another experiment, $\mu_0 H_m$ was fixed at 0.15 mT, and f was varied continuously up to 20 kHz. In such a low-field region, the hysteresis loss Q_h, which is proportional to ${H_m}^3$, is negligible, and the coupling loss Q_c is dominant. In general, the coupling loss per cycle of the sinusoidal field change is expressed as follows:

$$Q_c = A_c' \frac{\mu_0 H_m^2}{2} \cdot \frac{2\pi f \tau_c}{(2\pi f \tau_c)^2 + 1}, \tag{3}$$

where A_c' and τ_c are a geometry factor determined by the conductor geometry and the coupling time constant, respectively [29, 30, 33]. Note that the unit of A_c' is m^2, because the unit of Q_c is J m^{-1}. If Q_c is plotted against f, it reaches its peak at the frequency f_c:

$$f_c = 1/2\pi\tau_c. \tag{4}$$

In this study, we refer to this as the characteristic frequency. Filaments decouple electromagnetically at frequencies that are sufficiently low compared to the characteristic frequency f_c. By fitting equation (3) to the measured Q_m–f plot of a sample, which is approximately Q_c–f plot, we can determine both τ_c and A_c' of the sample using the least-squares method.

5. Results and discussion

5.1. Effect of spiral geometry on the reduction of magnetisation losses in copper-plated multifilament coated conductors

In this subsection, we compare the magnetisation losses of straight and spiral copper-plated multifilament and monofilament coated conductors.

Before comparing their magnetisation losses directly, we compare their coupling time constants τ_c, which we determined experimentally. As an example, we plot the measured

Table 1. Specifications of coated conductors used in experiments.

Coated conductor type	Conductor width (w_t)	Substrate thickness (t_{sub})	Number of filaments (n_f)	Filament width (w_f)[a]	Copper thickness per side (t_{Cu})[b]	Critical current (I_c)[c]
B2-a2	4 mm	30 μm	1	4 mm	20 μm	176.7 A
B2-b1	4 mm	30 μm	5	0.8 mm	40 μm	173.3 A
B2-b2	4 mm	30 μm	5	0.8 mm	20 μm	171.1 A
B2-b3	4 mm	30 μm	5	0.8 mm	10 μm	165.9, 166.4 A
B2-c1	4 mm	30 μm	10	0.4 mm	40 μm	Not available
B2-c2	4 mm	30 μm	10	0.4 mm	20 μm	154.0 A
B3-a1	2 mm	30 μm	1	2 mm	40 μm	67.8 A
B3-a2	2 mm	30 μm	1	2 mm	20 μm	69.1 A
B3-b1	2 mm	30 μm	3	0.67 mm	40 μm	35.4 A
B3-b2	2 mm	30 μm	3	0.67 mm	20 μm	40.2 A
B3-c1	2 mm	30 μm	5	0.4 mm	40 μm	33.8 A

[a] w_f is given as w_t divided by n_f.
[b] Copper covers the entire periphery of each coated conductor.
[c] These values were measured at 77 K at SuperPower Inc. The separation of the voltage taps is 3.1 m, and the criterion of the critical current is 100 μV m^{-1}.

Table 2. Specifications of spiral copper-plated coated conductors and reference straight copper-plated coated conductors for magnetisation loss measurements.

Coated conductor type	Conductor (tape) length (l_t)	Core diameter (D_c)	Spiral angle (α)	Spiral pitch (L_p)	Conductor (tape) length corresponding to $L_p/2$ ($L_{p1}/2$)	Number of conductors (tape) (n_t)	Critical current (I_c)[a]
Spiral copper-plated coated conductor							
B2-a2	174 mm	3 mm	55°	6.60 mm	5.75 mm	1	173.4 A
B2-b1	174 mm	3 mm	55°	6.60 mm	5.75 mm	1	167.4 A
B2-b2	174 mm	3 mm	55°	6.60 mm	5.75 mm	1	158.4 A
B2-b3	174 mm	3 mm	55°	6.60 mm	5.75 mm	1	161.5 A
B2-c1	174 mm	3 mm	55°	6.60 mm	5.75 mm	1	140.6 A
B2-c2	174 mm	3 mm	55°	6.60 mm	5.75 mm	1	168.6 A
B3-a1	174 mm	3 mm	55°	6.60 mm	5.75 mm	2	67.6, 67.9 A
B3-a2	174 mm	3 mm	55°	6.60 mm	5.75 mm	2	72.3, 70.3 A
B3-b1	174 mm	3 mm	55°	6.60 mm	5.75 mm	2	42.1, 42.7 A
B3-b2	174 mm	3 mm	55°	6.60 mm	5.75 mm	2	59.6, 55.7 A
B3-c1	174 mm	3 mm	55°	6.60 mm	5.75 mm	2	39.3, 38.2 A
B2-a2	174 mm	5 mm	55°	11.0 mm	9.59 mm	2	176.7, 176.1 A
B2-b1	174 mm	5 mm	55°	11.0 mm	9.59 mm	2	167.2, 161.6 A
B2-b2	174 mm	5 mm	55°	11.0 mm	9.59 mm	2	159.5, 160.9 A
B2-b3	174 mm	5 mm	55°	11.0 mm	9.59 mm	2	173.4, 170.1 A
B2-c1	174 mm	5 mm	55°	11.0 mm	9.59 mm	2	137.6, 140.4 A
B2-c2	174 mm	5 mm	55°	11.0 mm	9.59 mm	2	162.6, 157.4 A
Straight copper-plated coated conductor							
B2-a2	150 mm	N/A	N/A	N/A	N/A	N/A	176.7 A[b]
B2-b2	150 mm	N/A	N/A	N/A	N/A	N/A	171.1 A[b]
B2-c2	150 mm	N/A	N/A	N/A	N/A	N/A	138.9 A

[a] These values were measured at 77 K for each coated conductor unless otherwise noted. The critical current of each spiral coated conductor was measured before winding spirally. The criterion of the critical current is 100 μV m^{-1}.
[b] These values were measured at 77 K at SuperPower Inc. The separation of the voltage taps is 3.1 m, and the criterion of the critical current is 100 μV m^{-1}.

magnetisation losses Q_m against frequency f for the spiral 10-filament coated conductor B2-c2 (D_c = 3 mm) in figure 8 where $\mu_0 H_m$ was fixed at 0.15 mT. From such a plot for each sample, we determined the coupling time constant τ_c and the geometry factor A_c' for the sample using the method explained in section 4. Table 3 lists τ_c, f_c, and A_c' of the spiral and straight 5-filament coated conductors B2-b2 and 10-filament coated conductors B2-c2. As listed in tables 2 and 3, the conductor length L_t of the straight coated conductors was 150 mm, and that of the spiral coated conductors was 174 mm. The experimentally determined coupling time constants τ_c of the spiral copper-plated multifilament coated conductors are much smaller than those of straight copper-plated multifilament coated conductors, even though L_t of the spiral conductors is larger

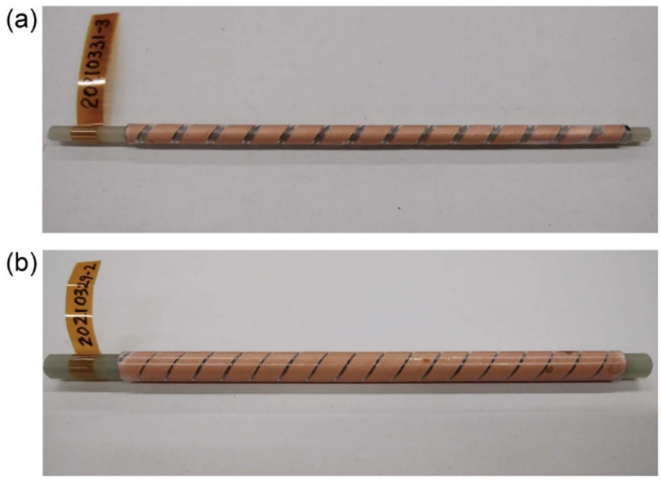

Figure 6. Pictures of spiral copper-plated multifilament coated conductors: (a) one 4 mm wide coated conductor wound spirally on a 3 mm core and (b) two 4 mm wide coated conductors wound spirally on a 5 mm core.

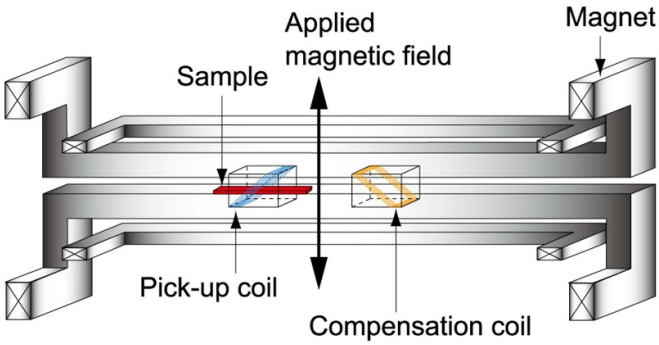

Figure 7. Schematic view of ac loss measurement system, with which we measured magnetisation losses at 77 K [16, 31, 32].

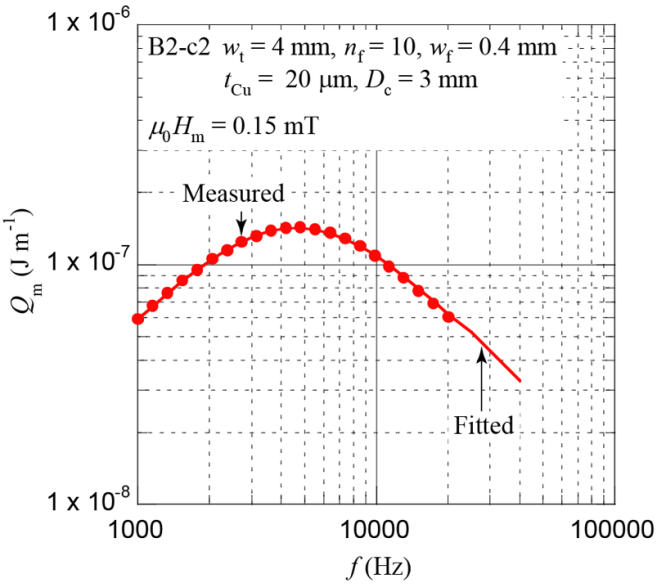

Figure 8. Measured magnetisation losses Q_m plotted against frequency f for the 10-filament coated conductor B2-c2 ($D_c = 3$ mm).

than that of the straight conductors. In straight copper-plated multifilament coated conductors, L_t determines their coupling time constants, which are proportional to the square of L_t [16]. Meanwhile, in spiral copper-plated multifilament coated conductors, $L_{p1}/2$ (=5.75 and 9.59 mm when $D = 3$ and 5 mm, respectively) determines their coupling time constants, which are much shorter than L_t (=174 mm) and independent of L_t.

In figure 9, we compare the magnetisation losses of various straight and spiral copper-plated coated conductors (monofilament B2-a2, 5-filament B2-b2, and 10-filament B2-c2, all with 20 μm thick copper) subjected to an ac transverse magnetic field whose amplitude $\mu_0 H_m$ is 100 mT and frequency f is 65.44 Hz. Looking at the magnetisation losses of the straight coated conductors, the magnetisation losses of the monofilament coated conductor (B2-a2, with $n_f = 1$) and multifilament coated conductors (B2-b2 with $n_f = 5$, and B2-c2 with $n_f = 10$) are almost the same. Filaments coupled electromagnetically in the straight B2-b2 and the straight B2-c2 at 65.44 Hz, which was remarkably larger than their f_c (7.91 and 10.3 Hz, respectively). Because coupled filaments behaved as a monofilament, the magnetisation losses of the straight B2-b2 and the straight B2-c2 at 65.44 Hz were at the same level as that of the monofilament coated conductor B2-a2. In practical applications, coated conductors are much longer than 150 mm, and magnetisation losses cannot be reduced using straight copper-plated multifilament coated conductors. On the contrary, when comparing spiral coated conductors, the magnetisation loss decreases with increasing number of filaments n_f, that is, with decreasing filament width w_f. The magnetisation loss of the spiral 10-filament coated conductor B2-c2 is approximately 15% of that of the spiral monofilament coated conductor B2-a2. This must be due to a small τ_c of the spiral B2-c2: the corresponding f_c, 4.60 kHz, is much higher than the frequency of the applied magnetic field, 65.44 Hz. The reason for Q_m of the spiral monofilament coated conductor B2-a2 being smaller than Q_m of the corresponding straight monofilament coated conductor B2-a2 could be the rotation of the tape face against the magnetic field in the spiral case. Because the magnetisation loss of a coated conductor is dominated by the applied magnetic field component normal to the tape face [34, 35], the rotation of the tape face in a spiral coated conductor could reduce the magnetisation loss. Finally, note that the magnetisation loss of the spiral 10-filament coated conductor B2-c2 is only 7% of that of the straight 10-filament coated conductor B2-c2 as well as that of the straight monofilament coated conductor B2-a2. This magnetisation loss reduction could be effective in longer multifilament coated conductors, because their coupling time constants are determined by the spiral pitch and independent of the overall length.

5.2. Magnetisation losses of a typical spiral copper-plated multifilament coated conductor and separating into hysteresis losses and frequency-dependent loss components

Figure 10 shows the measured magnetisation losses Q_m of the spiral 10-filament coated conductor B2-c2 ($D_c = 3$ mm),

Table 3. Coupling time constant τ_c, characteristic frequency f_c ($=1/2\pi\tau_c$), and geometry factor A_c' of straight and spiral copper-plated multifilament coated conductors.

	Straight	Spiral
Conductor (tape) length l_t	150 mm	174 mm
Core diameter D_c	N/A	3 mm
Spiral angle α	N/A	55°
B2-b2	Conductor width $w_t = 4$ mm, number of filaments $n_f = 5$, copper thickness per side $t_{Cu} = 20$ μm	
Coupling time constant τ_c	20.1 ms	47.3 μs
Characteristic frequency f_c	7.91 Hz	3.36 kHz
Geometry factor A_c'	6.45×10^{-5} m^2	2.80×10^{-5} m^2
B2-c2	Conductor width $w_t = 4$ mm, number of filaments $n_f = 10$, copper thickness per side $t_{Cu} = 20$ μm	
Coupling time constant τ_c	15.4 ms	34.6 μs
Characteristic frequency f_c	10.3 Hz	4.60 kHz
Geometry factor A_c'	7.94×10^{-5} m^2	3.19×10^{-5} m^2

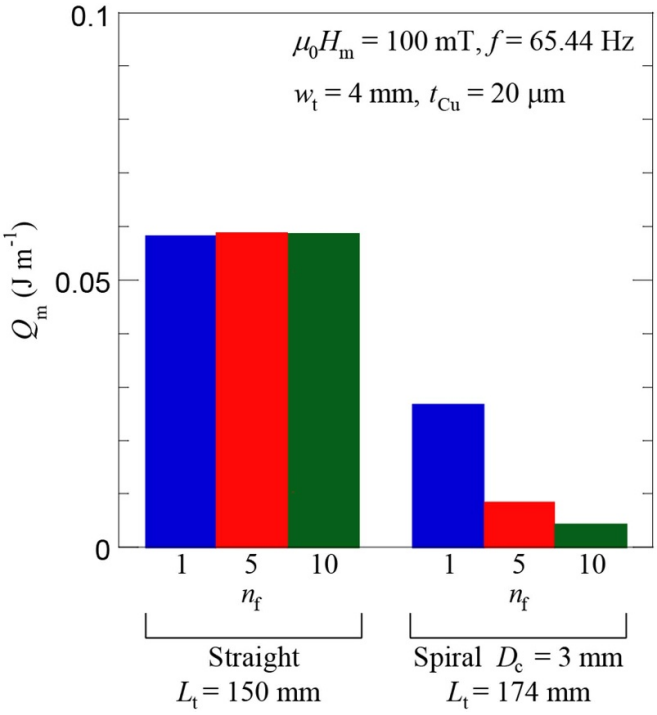

Figure 9. Magnetisation losses of various straight and spiral copper-plated coated conductors subjected to an ac transverse magnetic field whose amplitude $\mu_0 H_m$ is 100 mT and frequency f is 65.44 Hz. n_f denotes number of filaments, D_c denotes core diameter, and L_t denotes the length of the coated conductor, respectively. Coupling time constants of the spiral multifilament coated conductors whose number of filaments n_f are 5 and 10 are 47.3 and 34.6 μs, respectively, whereas those of the straight multifilament coated conductors whose number of filaments n_f are 5 and 10 are 20.1 and 15.4 ms, respectively.

which are plotted against field amplitude $\mu_0 H_m$. Here, we provide several analytical values for hysteretic magnetisation loss. The hysteresis loss in the coupled-filaments coated conductor is given as the hysteresis loss in a superconductor strip (or the monofilament coated conductor) with the same width and the same critical current [36]:

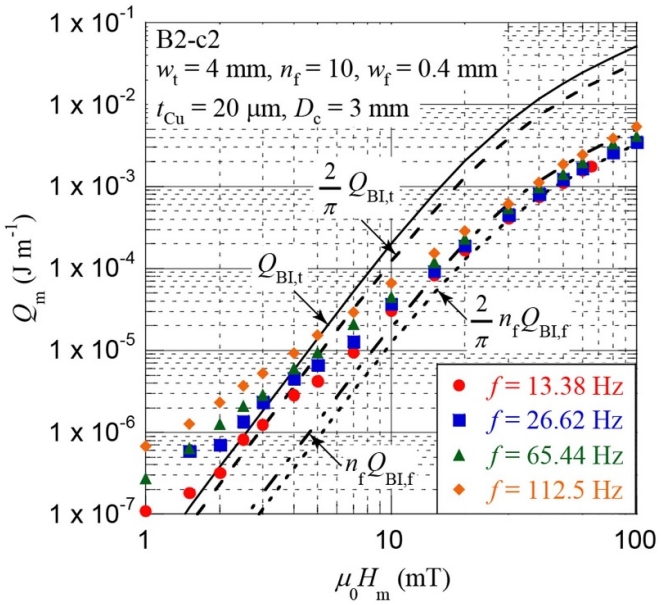

Figure 10. Measured magnetisation losses Q_m of the spiral 10-filament coated conductor B2-c2 ($D_c = 3$ mm) plotted against field amplitude $\mu_0 H_m$, together with analytical values of Brandt and Indenbom given by equations (5)–(9).

$$Q_{BI,t} = \mu_0 w_t I_c H_m g\left(\frac{H_m}{H_c}\right) = \frac{(\mu_0 H_m)^2 \pi w_t^2}{\mu_0}\left\{g\left(\frac{H_m}{H_c}\right) \Big/ \left(\frac{H_m}{H_c}\right)\right\}, \quad (5)$$

where,

$$g(x) = (2/x)\ln(\cosh x) - \tanh x, \quad (6)$$

$$H_c = I_c/\pi w_t, \quad (7)$$

w_t is the width of the coated conductor, and I_c is the critical current of the coated conductor. Assuming that the filament

width w_f and the critical current of each filament are w_t/n_f and I_c/n_f, respectively, the hysteresis loss in the decoupled-filaments coated conductor is given as:

$$n_f Q_{BI,f} = n_f \frac{(\mu_0 H_m)^2 \pi {w_f}^2}{\mu_0} \left\{ g\left(\frac{H_m}{H_c}\right) \Big/ \left(\frac{H_m}{H_c}\right) \right\}$$
$$= n_f \frac{(\mu_0 H_m)^2 \pi (w_t/n_f)^2}{\mu_0} \left\{ g\left(\frac{H_m}{H_c}\right) \Big/ \left(\frac{H_m}{H_c}\right) \right\}$$
$$\times \left(= \frac{1}{n_f} Q_{BI,t} \right). \quad (8)$$

Considering the rotation of the tape face in a spiral coated conductor mentioned in section 5.1, $Q_{BI,t}$ and $n_f Q_{BI,f}$ can be reduced as follows:

$$\left(\frac{1}{\pi/2} \int_0^{\pi/2} \cos\theta \mathrm{d}\theta \right) Q_{BI,t} = \frac{2}{\pi} Q_{BI,t}, \left(\frac{1}{\pi/2} \int_0^{\pi/2} \cos\theta \mathrm{d}\theta \right) n_f Q_{BI,f}$$
$$= \frac{2}{\pi} n_f Q_{BI,f}. \quad (9)$$

These analytical values are plotted in figure 10. When $\mu_0 H_m$ is high (higher than 20 mT, for example), the measured magnetisation losses Q_m are almost independent of frequency and are dominated by hysteresis losses. In this high field region, the measured Q_m almost follows $n_f Q_{BI,f}$ and $\frac{2}{\pi} n_f Q_{BI,f}$, rather than $Q_{BI,t}$ and $\frac{2}{\pi} Q_{BI,t}$ even at $f = 112.5$ Hz. These experimental results clearly show that spiral geometry can decouple filaments and reduce magnetisation losses. When $\mu_0 H_m$ is low (lower than 20 mT, for example), frequency-dependent coupling and/or eddy current losses may increase the measured Q_m.

In figure 11, we plot the measured magnetisation losses Q_m of the spiral 10-filament coated conductor B2-c2 ($D_c = 3$ mm) against frequency f (symbols at 13.38, 26.62, 65.44, and 112.5 Hz) where $\mu_0 H_m = 5$, 10, 20, 50, and 100 mT. The measured Q_m apparently shows frequency dependence. By fitting equation (10) to the measured Q_m–f plot shown in figure 11 to determine the values of Q_h and k, we can separate the measured magnetisation loss into frequency-independent and frequency-dependent components:

$$Q_m = Q_h + kf; k \text{ is a constant} \quad (10)$$

where Q_h is the frequency-independent component, which is indeed the hysteresis loss, and kf is the frequency-dependent component, which contains the coupling loss and eddy current loss. In the following, kf is denoted as Q_m–Q_h. The curves in figure 11 are given by equation (10), with Q_h and k determined by the fitting.

5.3. Hysteresis loss characteristics

Here, we compare the hysteresis losses Q_h of various spiral copper-plated multifilament coated conductors listed in table 2. As shown in table 2, the critical currents of the samples

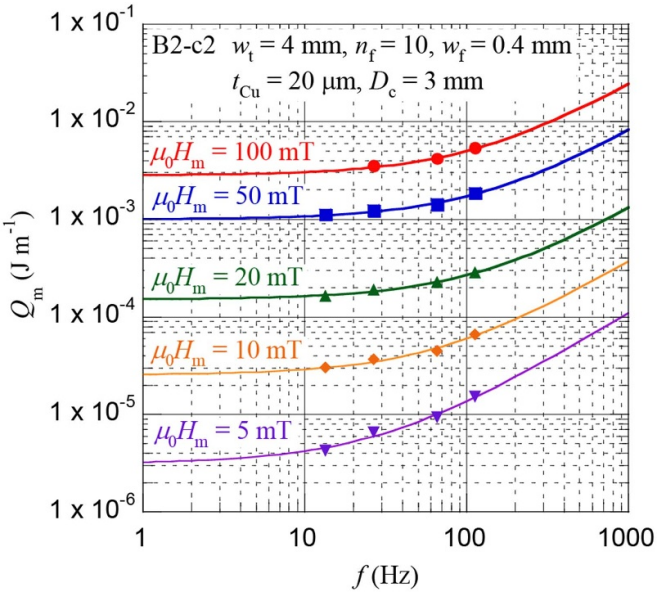

Figure 11. Measured magnetisation losses Q_m of the spiral 10-filament coated conductor B2-c2 ($D_c = 3$ mm) plotted against frequency f (symbols at 13.38, 26.62, 65.44, and 112.5 Hz) where $\mu_0 H_m = 5$, 10, 20, 50, and 100 mT, together with fitted curves by equation (10): $Q_m = Q_h + kf$; k is a constant.

were not always the same. To eliminate the influence of the difference in the critical currents, Q_h is normalised by the following Q_0:

$$Q_0 = \frac{(\mu_0 H_m)^2 \pi {w_t}^2}{\mu_0} \cdot \frac{w_0}{w_t}, w_0 = 4 \text{ mm}, \quad (11)$$

and, then, Q_h/Q_0 of the coated conductors with various critical currents are compared with one another. Ideally, the hysteresis loss per unit length in two pieces of decoupled 2 mm wide superconductor strip is half of that in one piece of 4 mm wide superconductor strip. The factor $\frac{w_0}{w_t}$ is included to represent this relationship. Consequently, the normalised analytical values $Q_{BI,t}$ and $n_f Q_{BI,f}$ are given as follows:

$$Q_{BI,t}/Q_0 = \left\{ g\left(\frac{H_m}{H_c}\right) \Big/ \left(\frac{H_m}{H_c}\right) \right\} \cdot \frac{w_t}{w_0}, w_0 = 4 \text{ mm}, \quad (12)$$

$$n_f Q_{BI,f}/Q_0 = \frac{1}{n_f} Q_{BI,t}/Q_0$$
$$= \frac{1}{n_f} \left\{ g\left(\frac{H_m}{H_c}\right) \Big/ \left(\frac{H_m}{H_c}\right) \right\} \cdot \frac{w_t}{w_0}, w_0 = 4 \text{ mm}. \quad (13)$$

Using this normalisation, when we plot $Q_{BI,t}/Q_0$ or $n_f Q_{BI,f}/Q_0$ against H_m/H_c, the plots for conductors with different critical currents but with identical geometries agree with each other. The normalised hysteresis loss $Q_{BI,t}/Q_0$ of two pieces of coated conductor whose width w_t is 2 mm becomes half of $Q_{BI,t}/Q_0$ of one piece of coated conductor whose width w_t is 4 mm. The normalised hysteresis loss $n_f Q_{BI,f}/Q_0$ of the n_f-filament coated conductor is reduced to $1/n_f$ times that of the monofilament coated conductor $Q_{BI,t}/Q_0$.

		w_t (mm)	n_f	w_f (mm)	t_{Cu} (μm)
◆	B2-a2	4	1	4	20
○	B2-b1	4	5	0.8	40
□	B2-b2	4	5	0.8	20
△	B2-b3	4	5	0.8	10
●	B2-c1	4	10	0.4	40
■	B2-c2	4	10	0.4	20

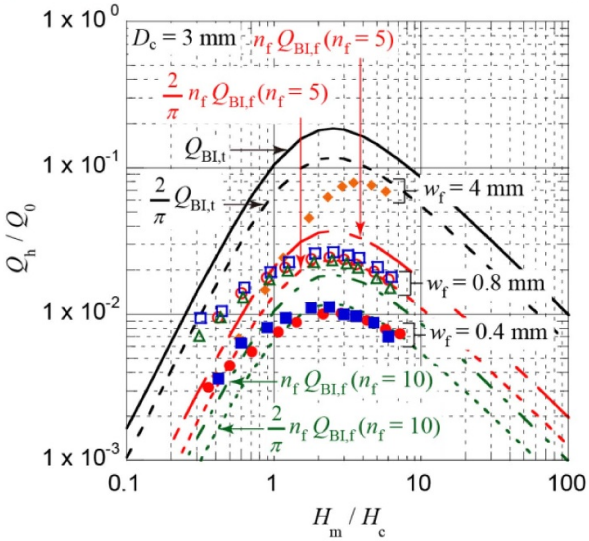

(a) D_c = 3 mm

		w_t (mm)	n_f	w_f (mm)	t_{Cu} (μm)
◆	B2-a2	4	1	4	20
○	B2-b1	4	5	0.8	40
□	B2-b2	4	5	0.8	20
△	B2-b3	4	5	0.8	10
●	B2-c1	4	10	0.4	40
■	B2-c2	4	10	0.4	20

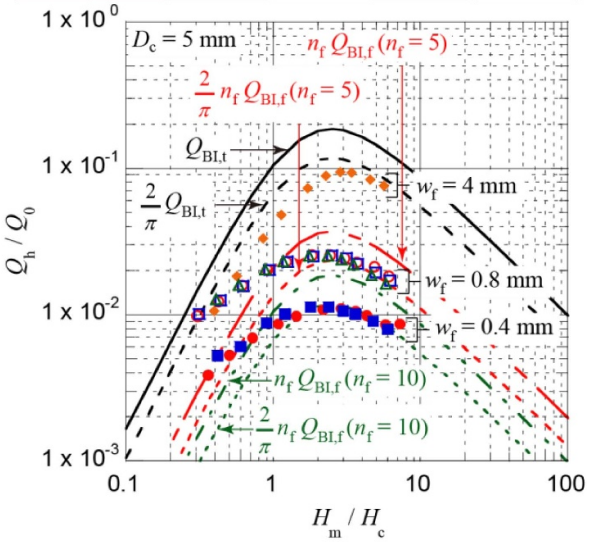

(b) D_c = 5 mm

Figure 12. Normalised hysteresis losses of various spiral copper-plated coated conductors and analytical values plotted against normalised magnetic field H_m/H_c where $1/Q_0$ is omitted in labels in the figures to save space: (a) $D_c = 3$ mm and (b) $D_c = 5$ mm.

In figure 12, we plot the normalised hysteresis losses of various spiral copper-plated coated conductors and analytical values against the normalised magnetic field H_m/H_c, where we fix the coated conductor width w_t at 4 mm and vary the filament width w_f (number of filaments n_f) and the copper thickness t_{Cu}. D_c is 3 mm in figure 12(a) and 5 mm in figure 12(b). Here, we focus on a high-field region, which is interesting from the viewpoint of practical applications. When $H_m/H_c > 1$, normalised measured hysteresis losses Q_h/Q_0 nearly follow the normalised $\frac{2}{\pi}n_f Q_{BI,f}/Q_0$, and Q_h/Q_0 of a coated conductor whose w_f is 0.4 mm are about half the Q_h/Q_0 of a coated conductor whose w_f is 0.8 mm. These results show the effect of decreasing the filament width to reduce hysteresis loss. Note that Q_h/Q_0 is almost independent of the copper thickness t_{Cu}: Q_h/Q_0 of coated conductors with an identical w_f but with different t_{Cu} are almost at the same level.

In figure 13, we plot the normalised hysteresis losses Q_h/Q_0 of spiral copper-plated coated conductors with various w_t, w_f (n_f), t_{Cu}, and D_c against filament width w_f. Q_h/Q_0 is almost proportional to the filament width.

5.4. Characteristics of frequency-dependent loss components

Next, we examine the frequency-dependent loss components. Figure 14 shows the frequency-dependent loss components Q_m–Q_h of various spiral copper-plated multifilament coated conductors plotted against frequency f when $\mu_0 H_m = 50$ mT. D_c is 3 mm in figure 14(a) and 5 mm in figure 14(b). The symbols represent the experimentally determined Q_m–Q_h, and the lines associated with the symbols are given by kf in equation (10), with k determined by fitting to the measured Q_m. The proportionality of Q_m–Q_h to f is reasonable, because Q_m–Q_h consists of the coupling loss Q_c and eddy current loss Q_e, both of which are proportional to frequency f when f is much smaller than f_c. In the figure, we also plot the eddy current loss $Q_{e,num}$, which was calculated numerically for spiral copper strips whose geometries are the same as those of the spiral-coated conductors. We calculated the eddy current losses in a spiral copper tape with a thickness and resistivity of 20 μm and 2×10^{-9} Ωm, respectively. Then, we multiplied by two to obtain $Q_{e,num}$, because both sides of a tape-shaped coated conductor are plated with copper. The calculated eddy current loss $Q_{e,num}$ is substantially smaller than the experimentally determined Q_m–Q_h, and it is acceptable to assume that Q_m–Q_h is dominated by the coupling loss Q_c.

In figure 15, Q_m–Q_h is plotted against the copper thickness t_{Cu}. It is natural that Q_m–Q_h increases with increasing copper thickness t_{Cu}, because the copper thickness t_{Cu} naturally increases the coupling loss and eddy current loss. The dependence of Q_m–Q_h (dominated by coupling loss Q_c) on the copper thickness t_{Cu} and our previous study on coupling time constants [21] suggest that copper resistivity dominates the transverse resistance. Therefore, it should be noted that coupling time constant and, then, coupling loss may increase with decreasing temperature because of the temperature dependence of the resistivity of copper. We have

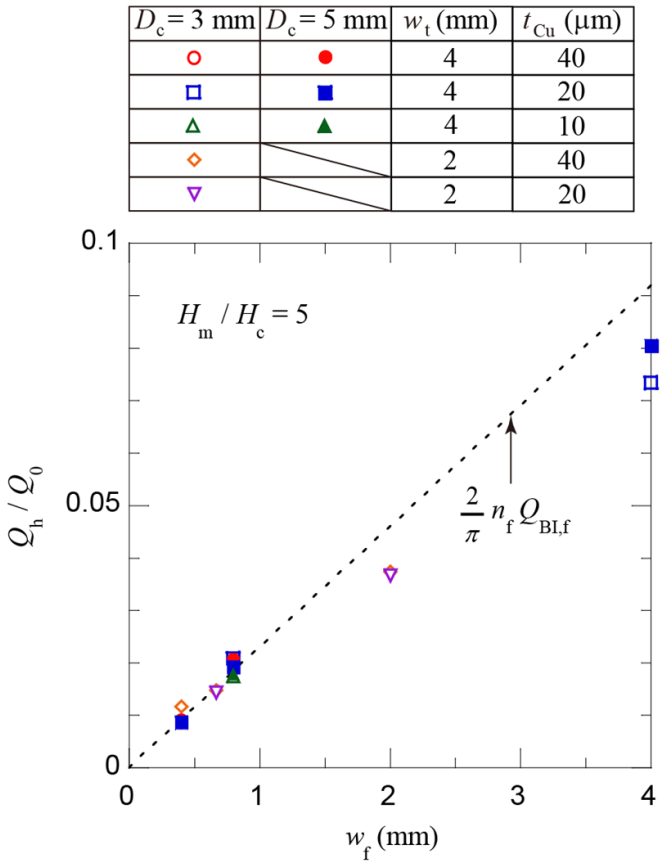

Figure 13. Normalised hysteresis losses Q_h/Q_0 of spiral copper-plated coated conductors with various w_t, w_f (n_f), t_{Cu}, and D_c plotted against filament width w_f.

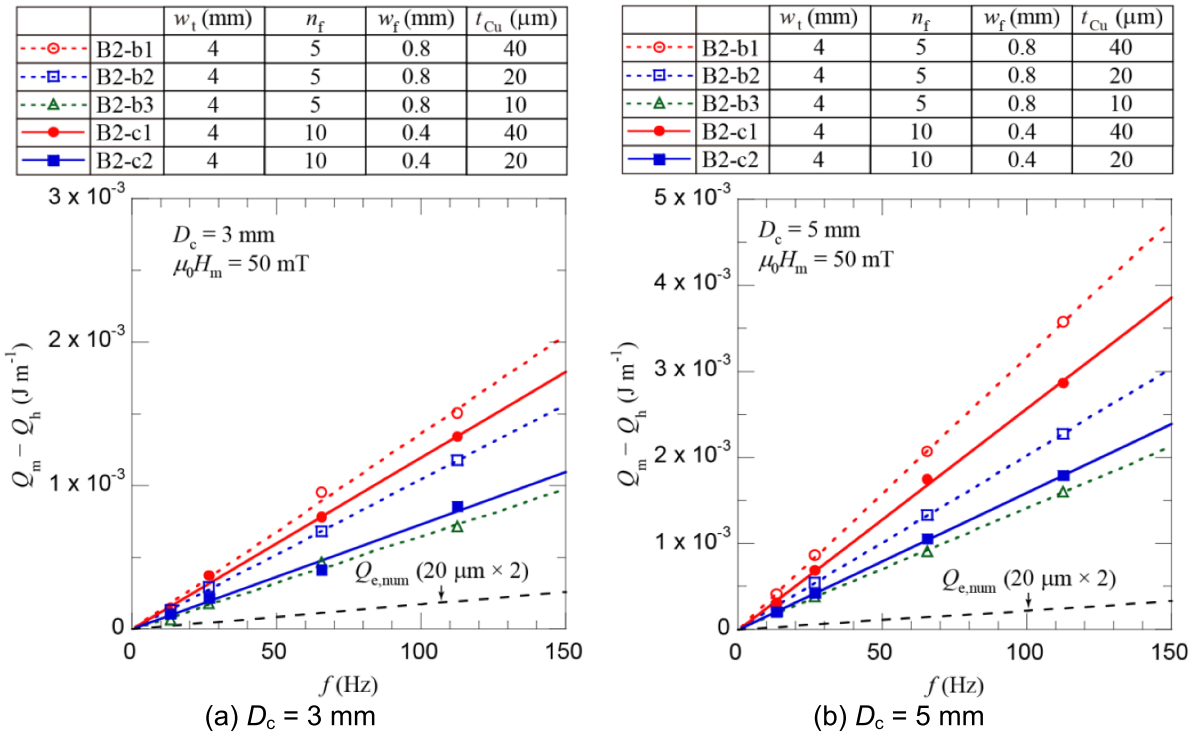

Figure 14. Frequency-dependent loss components Q_m–Q_h of various spiral copper-plated multifilament coated conductors plotted against frequency f when $\mu_0 H_m = 50$ mT where symbols representing experimentally determined Q_m–Q_h, and the lines associated with the symbols representing kf in equation (10), with k determined by fitting to the measured Q_m: (a) $D_c = 3$ mm and (b) $D_c = 5$ mm.

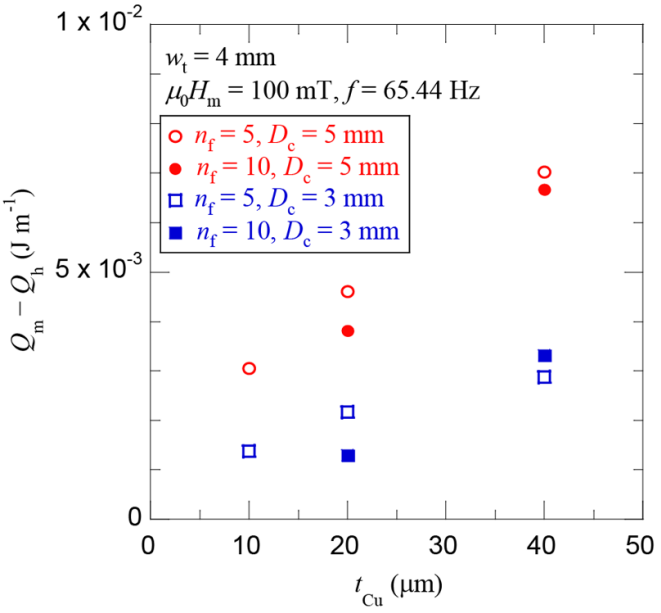

Figure 15. Frequency-dependent loss component Q_m–Q_h plotted against copper thickness t_{Cu}.

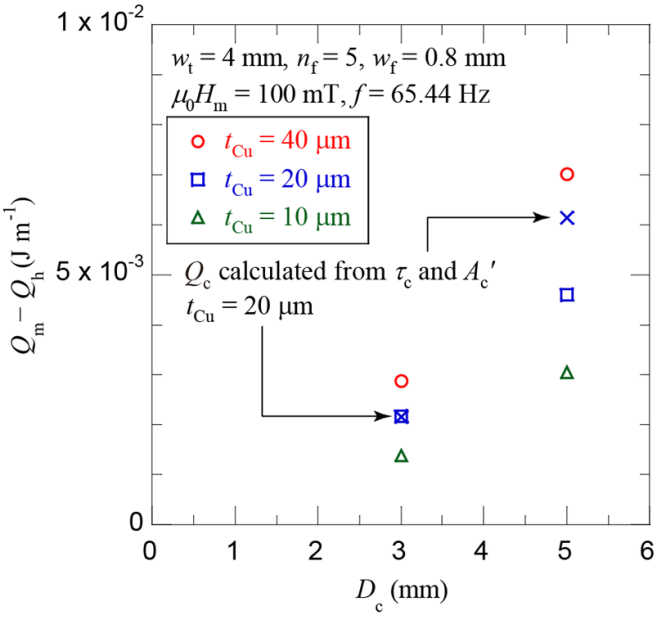

Figure 16. Frequency-dependent loss component Q_m–Q_h plotted against core diameter D_c, together with Q_c of the spiral 10-filament coated conductor B2-c2 ($t_{Cu} = 20$ μm) calculated by using equation (3) together with τ_c and A_c' listed in table 3.

to consider this temperature dependence of coupling time constant (characteristic frequency) when we operate the coil using the SCSC cable at a low temperature such as 4.2 K.

In figure 16, we plot Q_m–Q_h against core diameter D_c. The coupling time constant τ_c [21] and geometry factor A_c' decrease with decreasing core diameter D_c, as listed in table 3. Considering equation (3), it is understandable that Q_m–Q_h, which is dominated by the coupling loss Q_c, also decreases with decreasing core diameter D_c. The crosses in the figure show the coupling losses Q_c of the spiral 10-filament coated conductor B2-c2 ($t_{Cu} = 20$ μm) calculated using equation (3) together with τ_c and A_c' listed in table 3. Their dependence on the core diameter D_c qualitatively agrees with that of the measured values.

5.5. Comparison between hysteresis loss and frequency-dependent loss component

First, in figure 17(a), we compare the hysteresis loss Q_h and the frequency-dependent loss component Q_m–Q_h of the spiral 10-filament coated conductor B2-c2 ($D_c = 3$ mm), which are plotted with symbols against field amplitude $\mu_0 H_m$. In this spiral coated conductor with a 3 mm core, the hysteresis loss is larger than the frequency-dependent loss component, which is dominated by the coupling loss. In the figure, the dash–dot–dash line represents $n_f Q_{BI,f}$ given by equation (8), the broken line represents $\frac{2}{\pi} n_f Q_{BI,f}$ given by equation (9), and the solid line represents Q_c calculated using equation (3) together with τ_c and A_c'; listed in table 3. The experimentally determined Q_h agrees well with the hysteresis loss of the decoupled-filaments multifilament coated conductor $\frac{2}{\pi} n_f Q_{BI,f}$ considering the rotation of the tape face against the field direction. The experimentally determined Q_m–Q_h agrees well with the coupling loss Q_c calculated using equation (3) together with τ_c and A_c' listed in table 3.

Figure 17(b) shows similar plots for the spiral 10-filament coated conductor B2-c2 ($D_c = 5$ mm). In this conductor, the hysteresis loss and the frequency-dependent loss component are at almost the same level. The larger core diameter could increase the coupling loss. In this figure, again, the hysteresis loss agrees well with $\frac{2}{\pi} n_f Q_{BI,f}$ calculated using equation (9), whereas the frequency-dependent loss component is approximately two-thirds of Q_c calculated using equation (3) together with τ_c and A_c' listed in table 3. This error may be attributable to various uncertainties in the measurements as well as to fitting.

The experimental results suggest that we can estimate the hysteresis loss and coupling loss of an SCSC cable using equations (9) and (3) together with experimentally determined τ_c and A_c'. When using these equations to estimate the entire magnetisation loss of an SCSC cable, we must consider the following points:

- The hysteresis loss and coupling loss of the equations show different dependences on the amplitude and frequency of the applied magnetic field. Therefore, considering the expected amplitude and frequency of the applied magnetic field, we must identify which loss component is dominant when designing a copper-plated multifilament coated conductor.
- In addition to the geometry of a coated conductor, its critical current density and its transverse resistance between filaments influence its hysteresis loss and its coupling loss, respectively. In contrast, the critical current density and transverse resistance do not influence the coupling loss and hysteresis loss, respectively.

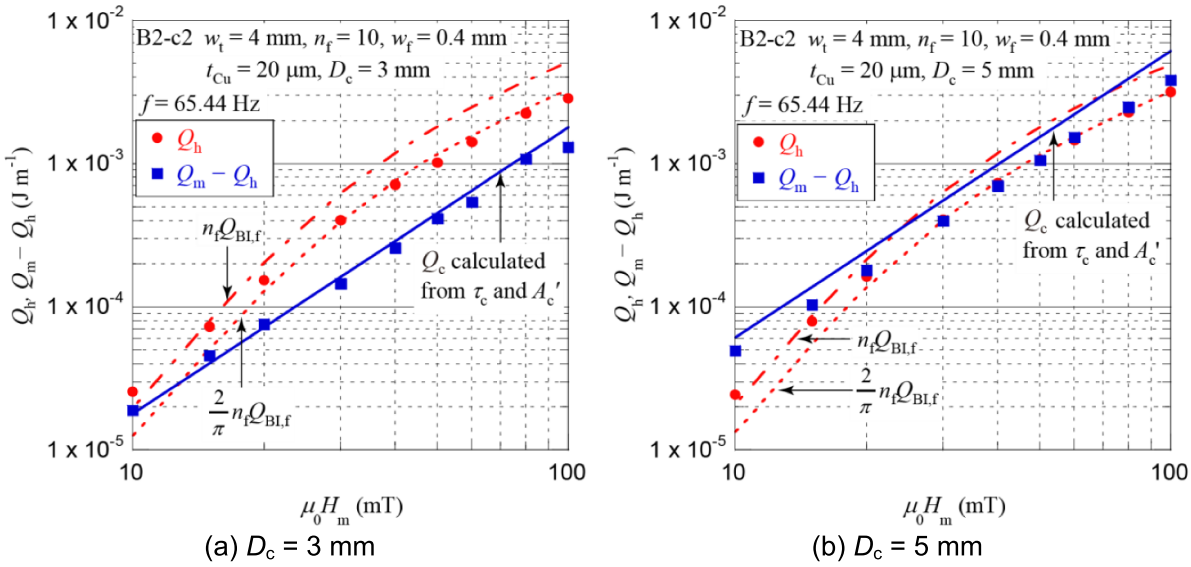

Figure 17. Hysteresis loss Q_h and frequency-dependent loss component Q_m–Q_h of the spiral 10-filament coated conductors B2-c2 ($t_{Cu} = 20$ μm) plotted with symbols against field amplitude $\mu_0 H_m$, together with dash–dot–dash line representing $n_f Q_{BI,f}$ given by equation (8), broken line representing $\frac{2}{\pi} n_f Q_{BI,f}$ given by equation (9), and solid line representing Q_c calculated by using equation (3) and τ_c and A_c' listed in table 3: (a) $D_c = 3$ mm and (b) $D_c = 5$ mm.

6. Conclusions

When a spiral copper-plated multifilament coated conductor, whose filaments are connected electrically by the copper layer, is subjected to an ac transverse magnetic field, its spiral geometry decouples filaments electromagnetically and effectively reduces its magnetisation loss. When a 4 mm wide, 10-filament coated conductor with 20 μm thick copper was wound spirally on a core whose diameter was 3 mm, the coupling time constant was 34.6 μs. Its magnetisation loss was only 7% of that of the same 10-filament coated conductor with a straight shape when they were subjected to an ac transverse magnetic field whose amplitude and frequency were 100 mT and 65.44 Hz, respectively. Because the coupling time constant is determined by the spiral pitch and is independent of the overall length of the coated conductor, the magnetisation loss reduction using spiral geometry is effective in long coated conductors in practical applications as well. The measured magnetisation loss of a spiral copper-plated multifilament coated conductor can be separated into a hysteresis loss and frequency-dependent loss component, which is mainly attributable to the coupling loss. The former can be reduced by decreasing the filament width, whereas the latter can be reduced by decreasing the copper thickness and core diameter. When designing a low-loss spiral copper-plated multifilament coated conductor such as the SCSC cable, we must identify which loss component is dominant, considering the operational conditions and the critical current density, which influences the hysteresis loss, and then we must choose proper conductor parameters such as filament width and copper thickness. Although their low engineering current density is a drawback of spiral coated conductors such as the SCSC cables and the CORC® wires, it can be increased by winding coated conductors with thinner substrate or those like STAR wires on cores with smaller diameters. Because the smallest filament width in this study (400 μm) is still much larger than the filament diameters of LTS wires, the ac loss could be much larger than LTS wires. However, the SCSC cables are still useful, because coated conductors have much larger temperature margins than those of LTS wires and can be operated at higher temperatures at which cooling systems are more efficient.

Data availability statement

All data that support the findings of this study are included within the article (and any supplementary files).

Acknowledgment

This work was supported by JST-Mirai Program Grant Number JPMJMI19E1, Japan.

ORCID iDs

Naoyuki Amemiya https://orcid.org/0000-0002-3000-864X
Yusuke Sogabe https://orcid.org/0000-0003-1692-629X

References

[1] Wulff A C, Abrahamsen A B and Insinga A R 2021 Multifilamentary coated conductors for ultra-high magnetic field applications *Supercond. Sci. Technol.* **34** 053003
[2] Grilli F and Kario A 2016 How filaments can reduce AC losses in HTS coated conductors: a review *Supercond. Sci. Technol.* **29** 083002

[3] Carr W J Jr and Oberly C E 1999 Filamentary YBCO conductors for AC applications *IEEE Trans. Appl. Supercond.* **9** 1475–8

[4] Amemiya N, Kasai S, Yoda K, Jiang Z, Levin G A, Barnes P N and Oberly C E 2004 AC loss reduction of YBCO coated conductors by multifilamentary structure *Supercond. Sci. Technol.* **17** 1464–71

[5] Sumption M, Collings E and Barnes P 2005 AC loss in striped (filamentary) YBCO coated conductors leading to designs for high frequencies and field-sweep amplitudes *Supercond. Sci. Technol.* **18** 122–34

[6] Levin G A, Barnes P N, Amemiya N, Kasai S, Yoda K and Jiang Z 2005 Magnetization losses in multifilament coated superconductors *Appl. Phys. Lett.* **86** 072509

[7] Amemiya N, Yoda K, Kasai S, Jiang Z, Levin G A, Barnes P N and Oberly C E 2005 AC loss characteristics of multifilamentary YBCO coated conductors *IEEE Trans. Appl. Supercond.* **15** 1637–42

[8] Majoros M, Glowacki B A, Campbell A M, Levin G A, Barnes P N and Polak M 2005 AC losses in striated YBCO coated conductors *IEEE Trans. Appl. Supercond.* **15** 2819–22

[9] Suzuki K, Matsuda J, Yoshizumi M, Izumi T, Shiohara Y, Iwakuma M, Ibi A, Miyata S and Yamada Y 2007 Development of a laser scribing process of coated conductors for the reduction of AC losses *Supercond. Sci. Technol.* **20** 822–6

[10] Tsukamoto O and Ciszek M 2007 AC magnetization losses in striated YBCO-123/Hastelloy coated conductors *Supercond. Sci. Technol.* **20** 974–9

[11] Abraimov D, Gurevich A, Polyanskii A, Cai X Y, Xu A, Pamidi S, Larbalestier D and Thieme C L H 2008 Significant reduction of AC losses in YBCO patterned coated conductors with transposed filaments *Supercond. Sci. Technol.* **21** 082004

[12] Iwakuma M *et al* 2009 Development of REBCO superconducting power transformers in Japan *Physica* C **469** 1726–32

[13] Kesgin I, Levin G A, Haugan T J and Selvamanickam V 2013 Multifilament, copper-stabilized superconductor tapes with low alternating current loss *Appl. Phys. Lett.* **103** 252603

[14] Vojenčiak M *et al* 2015 Magnetization ac loss reduction in HTS CORC® cables made of striated coated conductors *Supercond. Sci. Technol.* **28** 104006

[15] Godfrin A, Kario A, Gyuráki R, Demenčík E, Nast R, Scheiter J, Mankevich A, Molodyk A, Goldacker W and Grilli F 2017 Influence of the striation process and the thickness of the Cu-stabilization on the AC magnetization loss of striated REBCO tape *IEEE Trans. Appl. Supercond.* **27** 5900809

[16] Amemiya N, Tominaga N, Toyomoto R, Nishimoto T, Sogabe Y, Yamano S and Sakamoto H 2018 Coupling time constants of striated and copper-plated coated conductors and the potential of striation to reduce shielding-current-induced fields in pancake coils *Supercond. Sci. Technol.* **31** 025007

[17] Amemiya N, Sogabe Y, Yamano S and Sakamoto H 2019 Shielding current in a copper-plated multifilament coated conductor wound into a single pancake coil and exposed to a normal magnetic field *Supercond. Sci. Technol.* **32** 115008

[18] Šouc J, Gömöry F, Kováč J, Nast R, Jung A, Vojenčiak M, Grilli F and Goldacker W 2013 Low AC loss cable produced from transposed striated CC tapes *Supercond. Sci. Technol.* **26** 075020

[19] Li W, Sheng J, Zheng J, Wu Y, Guo C, Li Z and Jin Z 2021 Study on reducing magnetization loss in CORC cables by laser cutting technology *IEEE Trans. Appl. Supercond.* **31** 4802009

[20] Goo J, Han J W, Lee S, Kim W S, Choi K and Lee J K 2021 Magnetization loss of CORC with various configurations of 2G HTS strands *IEEE Trans. Appl. Supercond.* **31** 5901205

[21] Li Y, Kim D H, Inoue S, Yoshida Y, Machi T and Amemiya N 2020 Coupling time constant measurements of spirally-twisted striated coated conductors with finite transverse conductance between filaments *IEEE Trans. Appl. Supercond.* **30** 4703005

[22] van der Laan D C, Weiss J D and McRae D M 2019 Status of CORC® cables and wires for use in high-field magnets and power systems a decade after their introduction *Supercond. Sci. Technol.* **32** 033001

[23] Weiss J D, Mulder T, Kate H J T and van der Laan D C 2017 Introduction of CORC® wires: highly flexible, round high-temperature superconducting wires for magnet and power transmission applications *Supercond. Sci. Technol.* **30** 014002

[24] Kar S, Luo W, Yahia A B, Li X, Majkic G and Selvamanickam V 2018 Symmetric tape round REBCO wire with J_e (4.2K, 15T) beyond 450 Amm^{-2} at 15mm bend radius: a viable candidate for future compact accelerator magnet applications *Supercond. Sci. Technol.* **31** 04LT01

[25] Kar S, Luo W and Selvamanickam V 2017 Ultra-small diameter round REBCO wire with robust mechanical properties *IEEE Trans. Appl. Supercond.* **27** 6603204

[26] Amemiya N, Tominaga N, Sogabe Y, Yamano S and Sakamoto H 2017 Effect of striating coated conductors on reducing shielding-current-induced fields in pancake coils exposed to normal magnetic fields *25th Int. Conf. on Magnet Technology (MT-25) Tue-Af-Or18/106*

[27] Sogabe Y, Mizobata Y and Amemiya N 2020 Coupling time constants and ac loss characteristics of spiral copper-plated striated coated-conductor cables (SCSC cables) *Supercond. Sci. Technol.* **33** 055008

[28] Yan Y, Song P, Li W, Sheng J and Qu T 2020 Numerical investigation of the coupling effect in CORC cable with striated strands *IEEE Trans. Appl. Supercond.* **30** 4800305

[29] Willson M N 1983 *Superconducting Magnets* (Oxford: Oxford University) pp 174–81

[30] Iwasa Y 2009 *Case Studies in Superconducting Magnets Design and Operational Issues* 2nd edn (New York: Springer Science+Business Media) pp 406, 443

[31] Jiang Z and Amemiya N 2004 An experimental method for total AC loss measurement of high T_c superconductors *Supercond. Sci. Technol.* **17** 371–9

[32] Komeda T, Amemiya N, Tsukamoto T, Nakamura T, Jiang Z, Badcock R A, Bumby C, Long N J, Staines M and Buckley R G 2014 Experimental comparison of AC loss in REBCO Roebel cables consisting of six strands and ten strands *IEEE Trans. Appl. Supercond.* **24** 8200505

[33] Funaki K and Sumiyoshi F 1995 *Tashinsen to Doutai* (Tokyo: Sangyo Tosho) pp 34–35 (in Japanese)

[34] Amemiya N, Nishioka T, Jiang Z and Yasuda K 2004 Influence of film width and magnetic field orientation on AC loss in YBCO thin film *Supercond. Sci. Technol.* **17** 485–92

[35] Amemiya N, Jiang Z, Iijima Y, Kakimoto K and Saitoh T 2004 Total AC loss of YBCO coated conductor carrying AC transport current in AC transverse magnetic field with various orientations *Supercond. Sci. Technol.* **17** 983–8

[36] Brandt E H and Indenbom M 1993 Type-II-superconductor strip with current in a perpendicular magnetic field *Phys. Rev.* B **48** 12895–906